Visualizing and Quantifying Particular Matter (PM) Production and Concentration Trends at 30 Major U.S. Airports

Andy Eskenazi

1. Introduction

Commercial aviation emissions constitute an important source of aerosol production, both locally at airports but also globally due to transport mechanisms (Yim, 2015). The planetary impact of aerosols is multifaceted: on the one hand, because of their optical properties, aerosols can interact with light, potentially inducing a radiative forcing effect (Eastham, 2024). On the other hand, due to their ability to penetrate different parts of the human respiratory system, aerosols can deteriorate air quality (Saffaripour, 2020). While large aerosol particles (e.g., bigger than 2.5 microns in diameter) tend to get deposited in the nose, pharynx or larynx, smaller particles (e.g., smaller than 2.5 microns in diameter) can penetrate deeper, into the lungs, bronchioles and alveoli, resulting in respiratory and cardiovascular diseases, such as asthma, lung disfunctions, irregular heartbeats, and in extreme cases, premature mortalities (CAICE, 2020; Cui, 2024). Indeed, in a recent study conducted by Eastham et al. (2024), commercial aviation activities were found to cause up to 24,000 premature mortalities across the globe, every year.

In general, commercial aviation aerosol emissions consist of primary and secondary aerosol particles[1], as shown in **Figure 1** below. The former includes ultrafine (i.e., 15nm to 60nm in diameter) black carbon (BC), organic carbon (OC), and sulfur dioxide, SO_2, particles, all three of which are often referred to as non-volatile particulate matter, or nvPM (ICAOb, 2024; Bendtsen, 2021; Stacey, 2019; Lobo, 2015); the term nvPM is used to categorize particles that are solid at the engine's exhaust and do not volatize past 350º C (ICAOb, 2024; Saffaripour, 2020; Corbin, 2022). In general, BC and OC often result from unburnt jet fuel hydrocarbons in the jet engine's combustor (Saffaripour, 2020), while SO_2 originates due to the oxidation of the sulfur, S, present in jet fuel, often in the order of 0.4 g S/kg of fuel (IPCC, 2024). Meanwhile, the latter category (of aerosols) includes a variety of nitrate, NO_3^-, and sulfate, SO_4^{2-}, compounds, which are cumulatively referred to as volatile particulate matter, or vPM; the term vPM categorizes aerosol particles that form after the gaseous species emitted from the engine's combustor react with other species present in the environment and condense (Corbin, 2022).

As can be seen from the nvPM and vPM categorization, the difference between the two types of aerosols, primary and secondary, lies on the fact that the former are directly emitted from the aircraft's engine, while the latter form via interactions between precursor gaseous species coming from the jet engine's exhaust, namely nitrogen oxides, NO_x, and SO_2, and other molecules present in the atmosphere (Prashanth, 2022). For instance, as **Figure 1** shows, NO_2 can form nitric acid, HNO_3 (g) by interacting with a hydroxide molecule, OH, in the plume (IPCC, 2024). In its turn, HNO_3 (g) can react with an ammonia molecule, NH_3, to form ammonium nitrate, NH_4NO_3. Meanwhile, SO_2 can be oxidized by OH inside the engine to form a hydroxylsulfonyl radical, $HOSO_2$, which in turn can react with the emitted water vapor, H_2O (g), to form sulfuric acid, H_2SO_4 (l) (IPCC, 2024). While H_2SO_4 (l) is already an aerosol (given that it is suspended in the air when formed), it can continue reacting with two NH_3 molecules to form ammonium sulfate, $(NH_4)_2SO_4$. Overall, the formation of the nitrate or sulfate secondary aerosols will be dominated by the availability of NH_3 in the atmosphere (primarily from fertilizer emissions), given that both the SO_4^{2-} and NO_3^- anions will be competing for the ammonium NH_4^+ cation from the NH_3 present Prashanth, 2022). Thus, due to the inherent geographical distribution of ammonia sources (most notably, in farming lands), the formation of secondary aerosols will be location dependent (Levy, 2012; Yim, 2015).

[1] In general, when particulate matter (PM) is emitted into the atmosphere, it is suspended in the air, meaning that, by definition, PM could be understood as an aerosol (CAICE, 2020). With this context, the terms PM and aerosol particles are used interchangeably throughout this work.

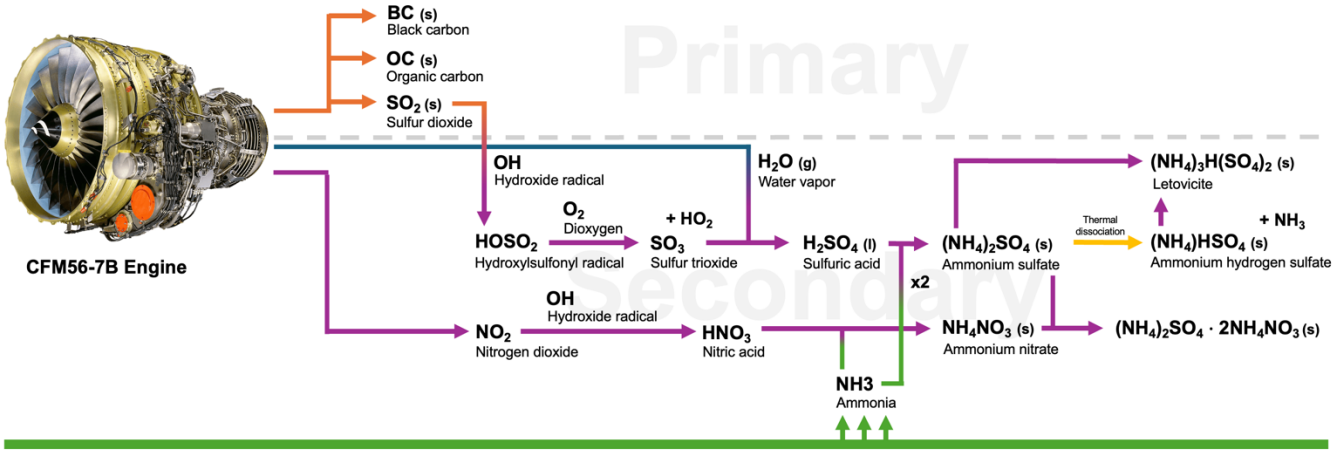

Figure 1: Formation of primary and secondary aerosols from the engine exhaust. Here, all molecules and compounds categorized as (s), for solid, or (l), for liquid, are aerosols, due to being suspended in the air. While many of the inorganic salts are categorized as (s), a rise in the specific location's relative humidity past the salt's deliquescence relative humidity (as defined by the location's temperature) could see these particles growing in size, absorbing atmospheric water, and transitioning to an aqueous (aq) state.

Currently, the standards imposed by the International Civil Aviation Organization (ICAO) do not address vPM formation; however, studies such as Corbin et al. (2022) have found that engine vPM emissions can be comparable in magnitude to nvPM, subject to NH_3 availability. Historically, the ICAO has regulated engine emissions of other gaseous compounds, primarily, NOx, which can act as a precursor for the formation of vPM. Only recently, after the meeting of the eleventh Committee on Aviation Environmental Protection (CAEP/11), has the ICAO introduced new standards to regulate PM emissions from aircraft engines, in particular nvPM emissions (ICAO, 2024b). Starting in 2020, instead of requiring engine manufacturers to report on the "Smoke" number (a dimensionless term quantifying emissions of carbonaceous particles due to incomplete combustion), ICAO now asks for the emission indices of nvPM at different thrust settings, corresponding to the four operation points of the landing-and-take-off (LTO cycle) - taxi, take-off, climb-out, and descent. In this context, LTO refers to the stage of the flight that takes place between the ground level and 3000 ft (914 m); while this altitude definition might seem low and arbitrary (representing only about 10% of typical cruising altitudes), the ICAO has established this bound specifically to regulate the local aircraft engine exhaust emissions. Indeed, due to the aircraft's proximity to the origin/destination airport during LTO, emissions in this stage of flight tend to have the most localized effects.

As the commercial aviation industry continues to grow, with an annual rate of 4.5% (ICAO, 2024), ***understanding, visualizing and quantifying the temporal and geospatial distribution of aerosol emissions becomes paramount***, so to assist communities in preparing policy to mitigate their air quality impacts. To this end, there exists an abundance of prior literature works that have examined the formation of aerosols at various temporal and spatial scales, either via experiments (e.g., directly measuring the $PM_{2.5}$ emitted from the engine exhaust), via modeling (e.g., using transport models such as GEOS-Chem to predict $PM_{2.5}$ inventories), or a combination of the two.

Studies that have experimentally measured either aircraft $PM_{2.5}$ produced at airports or $PM_{2.5}$ concentrations in areas in proximity to airports (i.e., quantifying aviation's local air quality impact) include: Hudda et al. (2014) and Shirmohammadi et al. (2017) at Los Angeles International Airport (LAX); Hudda et al. (2016) at Boston Logan International Airport (BOS); Hsu et al. (2012) at Rhode Island T. F. Green International Airport (PVD); and Lobo et al. (2015) at Atlanta Hartsfield Jackson International Airport (ATL). To start with, Hudda et al. (2014) examined $PM_{2.5}$ production at LAX using mobile monitoring sensors mounted on a vehicle, taking measurements at various locations to the east of the airport (i.e., in the primary direction the wind blows). Using meteorological data to model the transport of the produced aerosol particles, the study found a clear correlation between $PM_{2.5}$ production at LAX and the air quality

in the surrounding areas. This conclusion was later supported by Shirmohammadi et al. (2017), which using diffusion size classifier sensors, was able to determine mass and number concentrations of $PM_{2.5}$ at three locations surrounding LAX. Besides concluding, similarly to Hudda et al. (2014), that $PM_{2.5}$ concentrations at and nearby LAX were significantly higher than at the surrounding highways and neighborhoods, the study was also one of the first to compute average PM mass emission indices (EI) for each flight operation (i.e., landings or take-offs). In a later study, Hudda et al. (2016) repeated their LAX methodology at BOS, considering three PM measurement devices at distinct locations, within ~7km from the airport. The conclusion reached by the authors at BOS was similar to that previously reached at LAX: aviation-attributable PM represented a major cause for the deteriorated air quality at the three considered locations in Boston. However, this study also represented an improvement over the author's methodology, since it incorporated variabilities with regards to the time of the day and day of the week. Similarly in scope, Hsu et al. (2012), one of the earliest published studies, analyzed UFP concentrations due to aircraft LTO activity at PVD. Using a combination of in-site particle counters, as well as models to simulate wind speed and direction (to incorporate transport phenomena), the authors were able to demonstrate a statistically significant relationship between UFP concentrations in residential areas nearby PVD and flight activity at the airport. The study, however, recognized the difficulty in separating the contributions of aviation to the local PM concentrations from other local and background sources. Finally, Lobo et al. (2015), in an attempt to inform ICAO regulations on aircraft PM emissions, was one of the first studies to take direct measurements of PM emissions from specific turbofan engines, namely the JT8D (on the MD88), the PW2037 (on the B757), and the CF6-80 (on the B767). Conducting its trials at ATL using a custom-developed fast particulate spectrometer, the authors were able to calculate EIs (in the form of mg of nvPM/kg of fuel) specific for different thrust settings (ranging from 4% to 100% of the rated thrust).

Meanwhile, studies that have computationally modelled aircraft $PM_{2.5}$ (both from primary and secondary aerosol particles) alongside its transport, either from a country or global level, include: Cui et al. (2024) and Zhou et al. (2022) in China; Levy et al. (2021) and Woody et al. (2011) in the U.S.; and Yim et al. (2015) globally. To begin with, in China, the Cui et al. (2024) and Zhou et al. (2022) studies focused in developing a framework to analyze $PM_{2.5}$ concentration and production changes over time, respectively, although they differed in terms of the spatial and temporal granularity they each captured. The former utilized the Boeing Fuel Flow Method and historical flight data to compute nvPM at 175 airports in China, later feeding the results into a Gaussian diffusion method to resolve for the final geographical distributions of PM concentrations across the country (i.e., high spatial granularity). Meanwhile, the latter narrowed the scope to a single airport, Hangzhou Xiaoshan International Airport (HGH), and developed a data-driven approach to compute PM2.5 production based on engine-specific "Smoke" numbers[2], as reported to the ICAO by engine manufacturers. However, in contrast to Cui et al. (2024), Zhou et al. (2022) was able to determine fluctuations in nvPM production throughout the day, based on periods of high aircraft activity (i.e., high temporal granularity). In the U.S., Levy et al. (2012), and the preceding companion paper, Woody et al. (2011), computed LTO emissions from the country's top 99 airports. Using a chemistry-transport model incorporating inventories of precursor gaseous species (e.g., NH_3) across the country, Levy et al. (2012) developed a PM inventory across the 99 airports, capturing aircraft type and operation mode. The companion study, Woody et al. (2011), used a similar methodology to instead determine the changes in the country's $PM_{2.5}$ concentrations due to aviation. Overall, the study found that on average, civil aviation activity at the 99 airports was responsible for increasing the $PM_{2.5}$ concentrations by 3.2 ng/m^3. Finally, on a global scale, Yim et al. (2015), in a similar fashion to Woody et al. (2011), modelled the global changes in $PM_{2.5}$ concentrations due to civil aviation LTO operations at 968 airports across the globe. Using a chemical-transport with 4 x 5-degree resolution cells, as well as an EI of 30 mg/kg of fuel for BC and OC, and ICAO-defined emission factors for other precursor gaseous species (to model secondary aerosol particle formation), the study found that, on average, aviation could perturbate $PM_{2.5}$ concentrations globally by 6.2 ng/m^3 annually. However, in a 20km radius from the studied airports,

[2] The "Smoke" number was a metric developed by the ICAO in an attempt to regulate engine black smoke released in the exhaust plume. Although this metric is not particularly suitable for quantifying PM production, proxy models, based on experimental data, were developed to approximate $PM_{2.5}$ from this number.

aviation could increase the $PM_{2.5}$ concentrations by as much as 44.2 ng/m^3 on average (and in Asia, by as much as 74.1 ng/m^3).

As can be seen from the review of prior studies examining the formation of aerosols at various temporal and spatial scales, PM production at airports can be a major driver of both local and global air quality. However, these studies evidence that there exists a gap between the experimental works, which are granular in measurements but limited in temporal and geographical scope, and the computational works, which are able to capture variations across time and space, but are limited in granularity (i.e., cell resolution) due to computational capabilities. The present study is an attempt to bridge this gap, proposing an open-source data-driven tool that leverages experimental engine nvPM production EIs data recently tabulated in ICAO databases with global satellite data concerning PM2.5 concentrations at a 0.1 x 0.1-degree resolution. This tool serves a dual purpose: first, it enables **visualizing and quantifying**, for 30 major U.S. airports[3], **local nvPM production trends between 2009 and 2019** (before the COVID-19 pandemic). Second, it allows for **comparisons with the local $PM_{2.5}$ concentrations**, as well as the number of **flight operations** in the same period. While this work applies the tool to examine PM at airports in the U.S. (due to the availability of open-source data concerning flight activity), it can be easily extended to other regions of the world. The goal is that by providing an open-source package, **this work can help both better educate the public about the local air quality impact of aviation, as well as inform policy to precisely mitigate this impact**. The current version of the tool only focuses on primary aerosol particles, nvPM. As Corbin et al. (2022) points out, because vPM formation depends on the local atmospheric conditions, these aerosol particles are more difficult to model (especially with open-source data), so these were excluded from the analysis. Additionally, the geographical focus of the tool is local, at each airport, rather than global. As the reviewed literature conclusively agreed, aerosol particle numbers at or near airports tend to be higher than at surrounding locations (Stacey, 2019). Hence, people working at airports or in urban areas near airports are at an increased exposure risk to ultrafine particles (Stacey, 2019; Bendtsen, 2021), making this study space more relevant to analyze.

The remainder of this work is organized as follows: **Section 2** outlines the methodology, in particular the mathematical framework encoded in the developed tool to compute the produced nvPM and $PM_{2.5}$ concentrations at each of the 30 airports. **Section 3** presents the results, and focuses on three case study airports to illustrate temporal and spatial differences between them. Finally, **Section 4** delivers this work's conclusion and future work recommendations.

2. Methodology

The following section is split into two sub-parts, each concerned with detailing the framework for computing nvPM production and $PM_{2.5}$ concentrations ($[PM_{2.5}]$ hereafter) at each of the airports considered on this work.

2.1 Computing nvPM production

The framework for computing the production of nvPM at the 30 major U.S. airports considered on this work can be seen graphically in **Figure 2** below. In essence, this data-driven framework is enabled by leveraging the publicly available U.S. Bureau of Transportation Statistics (BTS) Form 41 T-100 Segment dataset (BTS, 2024) as well as the International Civil Aviation Organization's (ICAO) Aircraft Engine Emissions Databank (AEED) (EASA, 2024).

From the Form 41 T-100 Segment dataset, it is possible to extract information about all domestic and international flights operated in the U.S. between 2009 and 2019, granular to the aircraft type, airline, month, number of departures, and origin and destination airport level. As an example, looking at the Boston (BOS) to Chicago (ORD) route, during the entirety of 2019, 7 different airlines across 16 different aircraft types operated a grand total of 7140 departures (or an average of almost 20 flights per day). Of

[3] These 30 airports were selected in terms of their number of domestic enplanements in 2019 (BTS, 2024). More information regarding these airports can be found on the online public repository.

these, the most popular aircraft type was the B737-800, operating 40% of all the departures (2861 flights) from BOS to ORD.

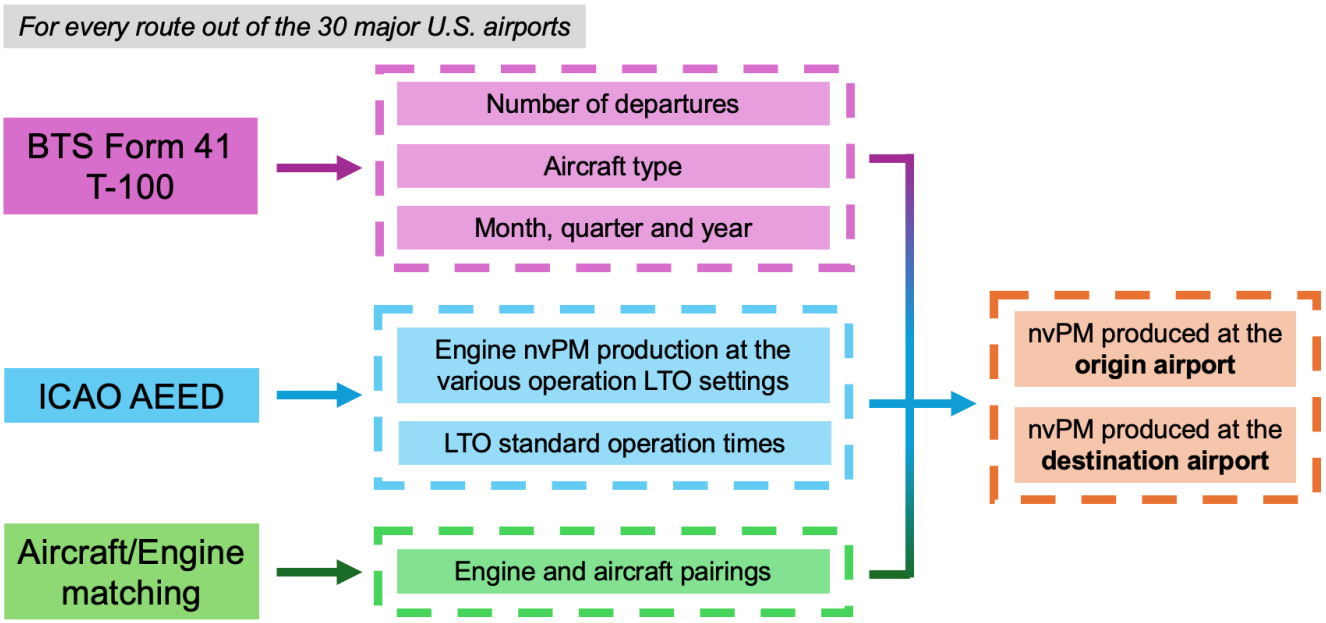

Figure 2: Framework for computing the production of nvPM at the origin and destination airport of each route. In this work, a total of 40 different aircraft types, equipped with 21 different engine options, were analyzed. The list of 30 U.S. airports considered on this work can be found on the online public repository.

Meanwhile, from the AEED, it is possible to obtain emission indices for the production of nvPM associated with different aircraft engines, at four different thrust settings (7%, 30%, 85% and 100% of the engine's rated thrust). As **Figure 3** and **Table 1** show below, these different settings roughly correspond to the typical thrust conditions the engines operate at during the landing-and-take-off (LTO) stage of flight, namely the taxi (7%), take-off (100%), climb (85) and approach (30%) operations. As an example, for the B737-800 mentioned above, equipped with two CFM56-7B engines, typical fuel flow values and nvPM emission indices can be found in **Table 1** below, extracted from the AEED. It should be mentioned, however, that neither the AEED nor the Form 41 dataset specify aircraft/engine pairings (i.e., the engines utilized by each aircraft type). As a result, this work approximated the pairings (e.g., B737-800 equipped with CFM56-7B engines) based on the airliner configurations U.S. airlines fly with today. More information about these aircraft/engine pairing approximations can be found on the online public repository.

Table 1: Fuel Flow, nvPM Emissions Index, and nvPM Flow for the CFM56-7B engine, as reported by the AEED (EASA, 2024). In parenthesis, next to each LTO Operation point, is the respective thrust setting (i.e., percentage of the rated thrust). The AEED exists as a result of engine manufacturers submitting to the ICAO their engine emissions performance profile (not only of nvPM production, but also of other pollutants such as Nitrogen oxides and Carbon monoxide, among others) at these different LTO thrust settings, in an attempt to meet regulation standards.

LTO Operation	**Fuel Flow F_{fuel}** (kg/s)	**Emission Index EI_{nvPM}** (mg nvPM/kg of fuel)	**nvPM Flow F_{nvPM}** (mg nvPM/s)
Take-off, T/O (100%)	0.896	33.5	30.0
Climb-out, C/O (85%)	0.746	22.7	16.9
Approach, App (30%)	0.268	1.0	0.268
Taxi, Idl (7%)	0.094	0.9	0.0846

For each of the four operation points of the LTO stage of flight, the ICAO establishes standard procedural times (ICAOb, 2024). For instance, for take-off, this is 42 seconds (0.7 minutes); for climb-out, 132s (2.2m); for approach, 240s (4m); and for taxi, 1560s (26m), accounting for both the departure and arrival portions. Hence, utilizing these standard times, the emission factors from AEED, and the flight information

from Form 41 T-100 Segment, it is possible to estimate the overall amounts of nvPM produced at each airport (for a particular time-period, e.g., month or year), as shown in **eq. (1)**, with the definition of each variable summarized on **Table 2** below.

$$\mathrm{nvPM_k} = \sum_{\mathrm{i_k} \in \mathrm{N_k}} \mathrm{dep_{i_k}} \cdot \left(42 \cdot \mathrm{F_{nvPM,i_k,T/O}} + 132 \cdot \mathrm{F_{nvPM,i_k,C/O}} + 780 \cdot \mathrm{F_{nvPM,i_k,Idl}}\right) + \sum_{\mathrm{j_k} \in \mathrm{M_k}} \mathrm{arr_{j_k}} \cdot \left(240 \cdot \mathrm{F_{nvPM,j_k,App}} + 780 \cdot \mathrm{F_{nvPM,j_k,Idl}}\right) \quad (1)$$

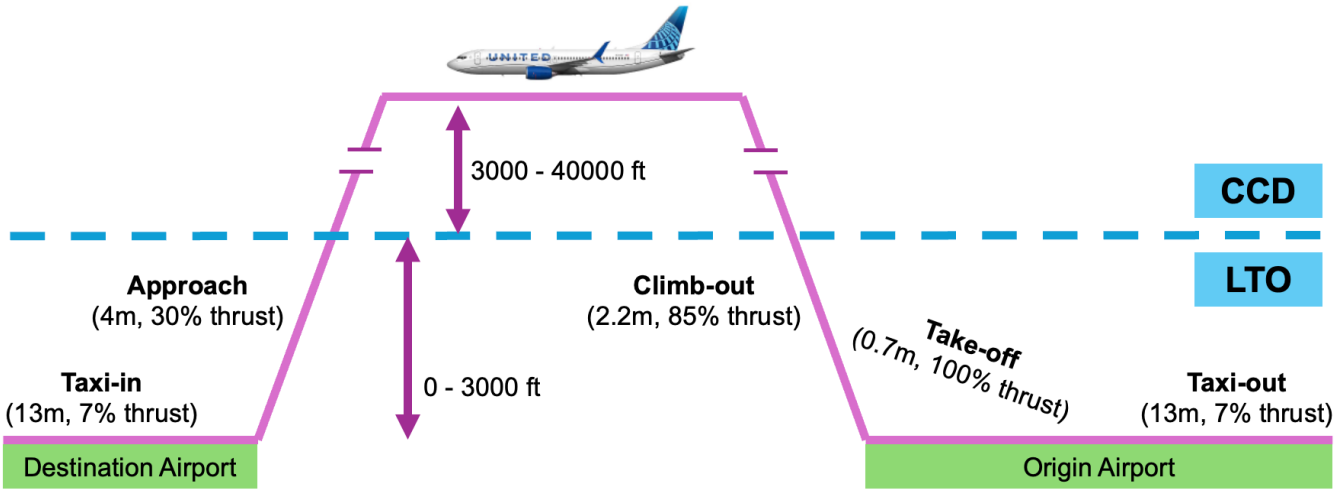

Figure 3: Different operation conditions during the landing-and-take-off (LTO) stage of flight. Between 3000 – 40000 ft, the stage is flight is often classified as Climb-Cruise-Descent (CCD), seeing different emission indices and a more global impact (as opposed to local).

Table 2: Variables utilized in eq. (1) for nvPM computations.

Variable	Definition
k $(\mathrm{k} \in \mathrm{A})$	k represents the airport in question, out of the 30 major airports contained in A. For example, $\mathrm{k} = \mathrm{BOS}$.
$\mathrm{i_k}$ $(\mathrm{i_k} \in \mathrm{N_k})$	$\mathrm{i_k}$ represents all the possible combinations of aircraft and routes out of airport k. In essence, this variable is used to index all departures operated out of k, across all US airlines, to a particular destination operated by a specific aircraft type. For example, when $\mathrm{k} = \mathrm{BOS}$, one of the $\mathrm{i_k}$ could be the flights to ORD on a B737-800, which in 2019 had $\mathrm{dep_{i_k}} = 2861$ departures. Another $\mathrm{i_k}$ could be flights to ORD, but operated on an E190, which in 2019 had $\mathrm{dep_{i_k}} = 1514$ departures. Meanwhile, $\mathrm{N_k}$ represents the set of aircraft and route combinations out of airport k.
$\mathrm{j_k}$ $(\mathrm{j_k} \in \mathrm{M_k})$	$\mathrm{j_k}$ represents the complementary definition to $\mathrm{i_k}$, and essentially consists of the combinations of aircraft and routes into airport k. For example, when $\mathrm{k} = \mathrm{ORD}$, one of the $\mathrm{j_k}$ could be the flights from BOS on a B737-800, which in 2019 had $\mathrm{arr_{j_k}} = 2861$ arrivals, while another $\mathrm{j_k}$ could be those arrivals into ORD also from BOS, but operated on an E190, which in 2019 had $\mathrm{arr_{j_k}} = 1514$ arrivals. Similarly to before, $\mathrm{M_k}$ denotes the set of aircraft and route pairings into airport k.
$\mathrm{F_{nvPM,i_k,T/O}}$	$\mathrm{F_{nvPM,i_k,T/O}}$ denotes the rate at which nvPM is generated during the take-off portion of the LTO stage of flight. Here, the index $\mathrm{i_k}$ is used to identify the specific aircraft operating the set of flights out of airport k towards a specific destination.

$F_{nvPM,i_k,C/O}$	$F_{nvPM,i_k,C/O}$ similarly denotes the rate at which nvPM is generated during the climb-out portion of the LTO stage of flight.
$F_{nvPM,i_k,Idl}$	$F_{nvPM,i_k,Idl}$ represents the rate at which nvPM is generated during the taxi portion of the LTO stage of flight, which takes place at both the departure and arrival airports.
$F_{nvPM,j_k,App}$	$F_{nvPM,j_k,Ap}$ finally denotes the rate of nvPM production during the approach portion of the LTO stage of flight. The index j_k is used to identify the specific aircraft operating the set of flights into airport k from a specific origin.

In general terms, **eq. (1)** can be interpreted as the "sum of two summations", where the first summation corresponds to the nvPM production from departing flights out of airport k and the second one denotes the nvPM production from flights arriving at the same airport. For instance, in 2019, the B737-800 departures from BOS to ORD would constitute:

$$\mathrm{nvPM}_{i_{ORD,2019,B737-800}} = 2861 \cdot \left(132[\mathrm{s}] \cdot 16.9\left[\frac{\mathrm{mg}}{\mathrm{s}}\right] + 780[\mathrm{s}] \cdot 0.0846\left[\frac{\mathrm{mg}}{\mathrm{s}}\right]\right) = 10.18\ \mathrm{kg\ nvPM} \quad (2)$$

Meanwhile, these same flights, which also represented arrivals into ORD from BOS, would contribute:

$$\mathrm{nvPM}_{j_{BOS,2019,B737-800}} = 2861 \cdot \left(240[\mathrm{s}] \cdot 0.268\left[\frac{\mathrm{mg}}{\mathrm{s}}\right] + 780[\mathrm{s}] \cdot 0.0846\left[\frac{\mathrm{mg}}{\mathrm{s}}\right]\right) = 0.37\ \mathrm{kg\ nvPM} \quad (3)$$

Here, the 10.18 kg of nvPM would contribute to the first summation (departures) of **eq. (1)**, while the 0.37 kg of nvPM would fall under the second summation (arrivals), although counting for different airports ($k = BOS$ and $k = ORD$, respectively). As can be seen from these example calculations, the amount of nvPM produced during take-off is significantly greater than that amount produced during landing, for the same flights operated with the same aircraft type. Not surprisingly, this is due to the high value of $F_{nvPM,i_k,T/O}$ and $F_{nvPM,i_k,C/O}$ relative to the other portions of the LTO stage of flight. Additionally, for both the origin and destination airport, the taxi time was assumed to be 780s (13m), an equal split of the standard ICAO-specified time. Now, although **eq. (1)** describes the absolute value of the nvPM produced at each airport, it is difficult to attribute from this quantity alone the major driving forces that may have caused production changes over time, e.g., changes in the number of operations (i.e., landings and take-offs) at an airport or improvements in engine technologies. To this end, to better compare and attribute changes of airport nvPM over time, a more useful metric would be to normalize **eq. (1)** by the total number of operations at the airport, as shown in **eq. (4)** below:

$$\mathrm{nvPM}_{k,ops} = \frac{\mathrm{nvPM}_k}{\sum_{i_k \in N_k} \mathrm{dep}_{i_k} + \sum_{j_k \in M_k} \mathrm{arr}_{j_k}} \quad (4)$$

As the results section will explore more in detail, for constant or increasing total number of operations at an airport (which has been the case during most of the 2009 – 2019 period), a decrease in $\mathrm{nvPM}_{k,ops}$ could be attributed to improvements in engine technology.

2.2 Computing $PM_{2.5}$ concentration ($[PM_{2.5}]$)

Meanwhile, the process for determining $[PM_{2.5}]$ is made possible by leveraging open-source data and code from the Atmospheric Composition Analysis Group (ACAG) at the University of Washington in St. Louis (Shen, 2024). The ACAG dataset consists of satellite geospatial measurements corresponding to

surface $PM_{2.5}$ concentrations in North America, available on a monthly and annual basis (as early as the year 2000 until 2022) on a 0.01-degree grid resolution.
The open-source code provided by the ACAG research group can be modified (as shown on the online public repository) so that the user can input any latitude and longitude, and extract average surface $[\mathrm{PM}_{2.5}]$ within a given resolution radius (defined in degrees) around these coordinates. To this end, the present study compiled representative latitude and longitudes for each of the 30 major U.S. airports considered in the analysis, as well as for reference cities close to each airport in question, to allow for $[\mathrm{PM}_{2.5}]$ comparisons between the two. The online public repository contains more details about the specific latitude and longitudes utilized for each airport, alongside the reference city chosen for comparison for each case.

3. Results

The above-described methodology can be implemented to construct the MATLAB tool available on this work's online public repository, which in its turn can be utilized to generate the figures featured in this section. These figures consist of four plots:

- **Upper left:** a bar plot comparison of the $[\mathrm{PM}_{2.5}]$ between the airport in question and the reference city, for a specific month and resolution radius, as well as the yearly average in each case for contextualization. Currently, the concentration results correspond to 2019, although other datasets from ACAG could be downloaded and utilized to calculate results for other years.
- **Upper right:** a map plot displaying the coordinate locations of the airport and its reference city, alongside the selected resolution radius.
- **Lower left:** a bar plot displaying the evolution of the monthly $\mathrm{nvPM}_{\mathrm{k,ops}}$ and the monthly number of flight operations (i.e., landings and take-offs) between 2009 and 2019, for the chosen airport k and the specific month.
- **Lower right:** a scatter plot for the average yearly $[\mathrm{PM}_{2.5}]$ against $\mathrm{nvPM}_{\mathrm{k,ops}}$, alongside a best fit line.

To use the tool, the user must specify a) an airport (out of the 30 options, using the standard three-letter code), b) a month (for $[\mathrm{PM}_{2.5}]$ comparisons between the airport and the reference city), and c) a resolution radius (to determine the area in which the $[\mathrm{PM}_{2.5}]$ is calculated).

The present study only displays the results for three airports case studies (for specific choices of months and resolution radii). As can be seen summarized in **Table 3** below as well as graphically in **Figure 4 – Figure 6**, these case studies are Boston Logan (BOS), Philadelphia International (PHL), and Phoenix Sky Harbor (PHX). These three airports were chosen due to displaying distinct results, justifying the need to examine PM trends from an airport-specific perspective. The results for all other 27 airports can be obtained by running the online public repository, for various choices of months and resolution radii.

Table 3: Summary of main trends in nvPM production and $[\mathrm{PM}_{2.5}]$ at three major U.S. airports.

Airport	Boston Logan	Philadelphia International	Phoenix Sky Harbor
Reference Month	November	September	August
Reference Resolution Radius	0.01 degrees	0.02 degrees	0.02 degrees
Monthly $[\mathrm{PM}_{2.5}]$ comparison	▪ BOS had a slightly higher $[\mathrm{PM}_{2.5}]$ than the reference city location, but the concentration levels were relatively low in both cases. ▪ This tendency did not remain true throughout	▪ PHL had a lower $[\mathrm{PM}_{2.5}]$ than the reference city location, a tendency that remained true for all other months beyond just the reference (September).	▪ PHX had a consistently higher $[\mathrm{PM}_{2.5}]$ than the reference city location, both in the reference month (August) and throughout the entire year.

	the entire year; in the summertime, $[PM_{2.5}]$ in the reference city exceed those of BOS, and the overall levels were higher. ▪ The average $[PM_{2.5}]$ for the entire year was higher than the concentrations in the reference month (November).	▪ Throughout the entire year, the average $[PM_{2.5}]$ was higher than the concentrations in September, both in PHL and the reference city location.	▪ The average yearly $[PM_{2.5}]$ was lower than in August, both in PHX and the reference city location. ▪ This is an expected result, since August is a month of high aviation activity.
Monthly $nvPM_{k,ops}$ evolution, between 2009 and 2019	▪ $nvPM_{k,ops}$ November levels have on average experienced a decrease, from 24.7 mg to 15.7 mg of nvPM per flight operation (i.e., landing and take-offs). ▪ During this same period, the number of November operations has mostly seen an increase, from 10,200 to 15,000. ▪ Decreases in $nvPM_{k,ops}$ could be attributed mostly to improvements in aircraft technology.	▪ $nvPM_{k,ops}$ September levels experienced an increase, followed by a decrease, overall seeing a decrease from 16.9 to 14.7 mg of nvPM per flight operation. ▪ During this same period, the number of September operations decreased from 12,000 to 9,400 until 2017, and then increased to 10,100. ▪ The changes in $nvPM_{k,ops}$ could be attributed to the changes in flight operations as opposed to improvements in aircraft technologies.	▪ $nvPM_{k,ops}$ August levels steadily decreased, from 15.4 to 9.6 mg of nvPM per flight operation. ▪ Meanwhile, the number of August operations also decreased steadily from 18,400 to 16,400. ▪ Thus, the changes in $nvPM_{k,ops}$ can be attributed primarily to decreases in flight operations.
Average yearly $[PM_{2.5}]$ against $nvPM_{k,ops}$, between 2009 and 2019	▪ The yearly average $[PM_{2.5}]$ and $nvPM_{k,ops}$ **did not show any clear relationship**. ▪ Even though the line of best fit shows a positive slope, the R^2 coefficient is low, at 0.15. ▪ It is not possible to attribute the average yearly nvPM production per operation at BOS as a driving factor of the concentration seen around the airport.	▪ The yearly average $[PM_{2.5}]$ and $nvPM_{k,ops}$ **showed a positive relationship**. ▪ The line of best fit had a medium-level R^2 coefficient of 0.47. ▪ The average yearly nvPM production per operation at PHL could be one driving factor behind $[PM_{2.5}]$ levels around the airport.	▪ The yearly average $[PM_{2.5}]$ and $nvPM_{k,ops}$ **showed a strong correlation**. ▪ The line of best fit had a high R^2 coefficient of 0.81. ▪ The average yearly nvPM production per operation at PHX could be one major driving factor behind $[PM_{2.5}]$ levels at PHX.

As can be seen, among the three case study airports, there were very distinct temporal and spatial differences in the nvPM production and $[PM_{2.5}]$ trends. As a result, conclusions can only be partially derived for specific airports, and not for all 30 major U.S. airports considered on this work at once. First, when comparing $[PM_{2.5}]$ levels between the airport and the reference city location, BOS, PHL and PHX saw monthly variations, both in trend and magnitude. Depending on the month, BOS $[PM_{2.5}]$ would exceed the reference city location concentration, but in the other two airports, the $[PM_{2.5}]$ would either always be lower at the airport (PHL) or higher (PHX). Second, when looking at the evolution of the monthly $nvPM_{k,ops}$ over time, all three airports saw similar trends, although the driving factor behind these were different. In BOS, while the $nvPM_{k,ops}$ decreased between 2009 and 2019, the number of operations increased – hence, improvements in engine technology could have played a major role influencing this result. Meanwhile, in both PHL and PHX, the decrease in $nvPM_{k,ops}$ mirrored a decrease in the number of flight operations, making it difficult to identify the impact of engine improvements in this trend. Finally, in terms of the relationship between the average yearly $[PM_{2.5}]$ against $nvPM_{k,ops}$, all three airports saw distinct correlations, with varying R^2 coefficients. In BOS, the R^2 value was relatively low, meaning that nvPM production from aircraft alone did not seem to influence the $[PM_{2.5}]$ seen in the immediate vicinity of this airport[4]. Meanwhile, in PHL and PHX, the R^2 values were higher, at 0.473 and 0.814, respectively, indicating that aircraft $nvPM_{k,ops}$ could have played a more significant role influencing the $[PM_{2.5}]$ measured around these airports. As a matter of fact, out of all the 30 major U.S. airports considered in this work, PHX showed the strongest correlation between $nvPM_{k,ops}$ and $[PM_{2.5}]$. However, more work would be merited to validate this relationship using field measurement $[PM_{2.5}]$ data.

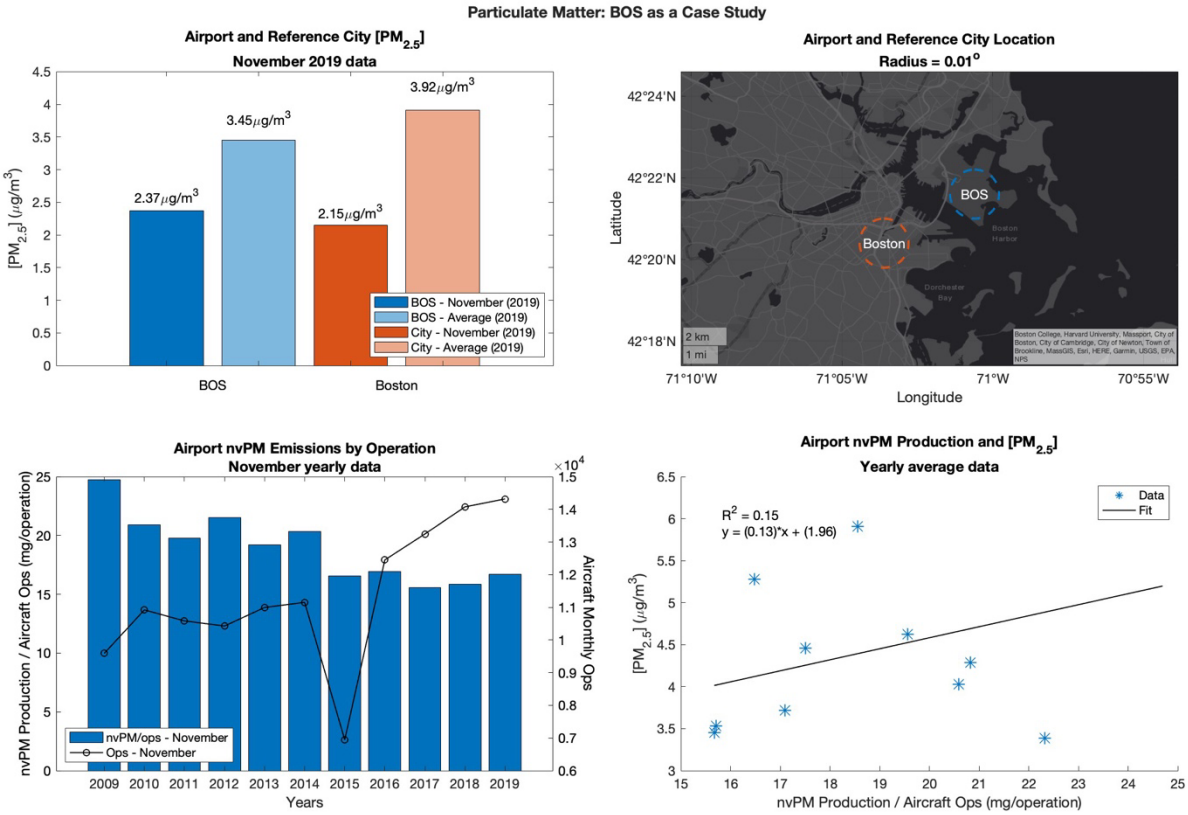

Figure 4: $nvPM_{k,ops}$ and $[PM_{2.5}]$ at BOS during 2009 and 2019. Here, the results on the upper and lower left plot correspond to November, while the $[PM_{2.5}]$ were calculated for a resolution radius of 0.01 degrees.

[4] In Hudda et al. (2016), the PM monitoring sensors were placed ~7km away from BOS, as opposed to being in close proximity to the airport, as evaluated within the $PM_{2.5}$ radii proposed in this work's tool. This difference in locations, in addition to the lack of transport modeling in this work, explains the disparities in results.

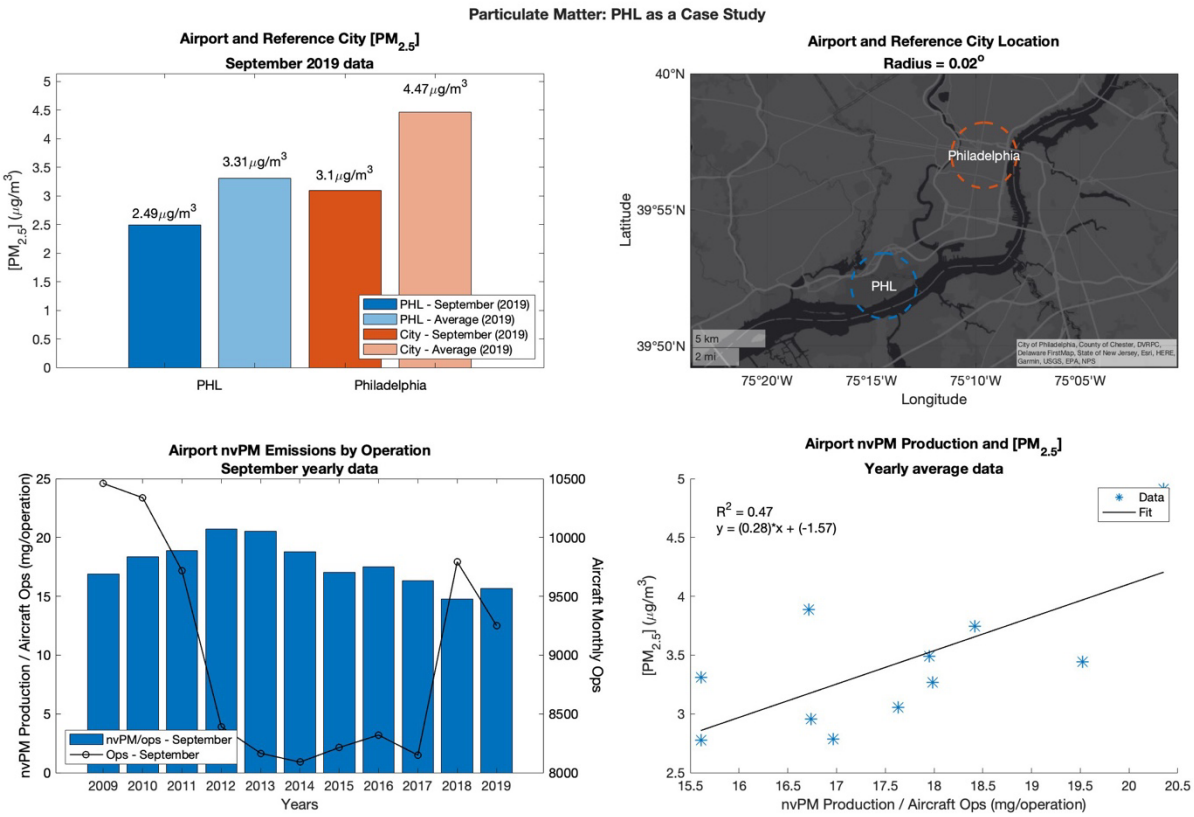

Figure 5: $\mathrm{nvPM_{k,ops}}$ and $[\mathrm{PM_{2.5}}]$ at PHL during 2009 and 2019. Here, the results on the upper and lower left plot correspond to September, while the $[\mathrm{PM_{2.5}}]$ were calculated for a resolution radius of 0.02 degrees.

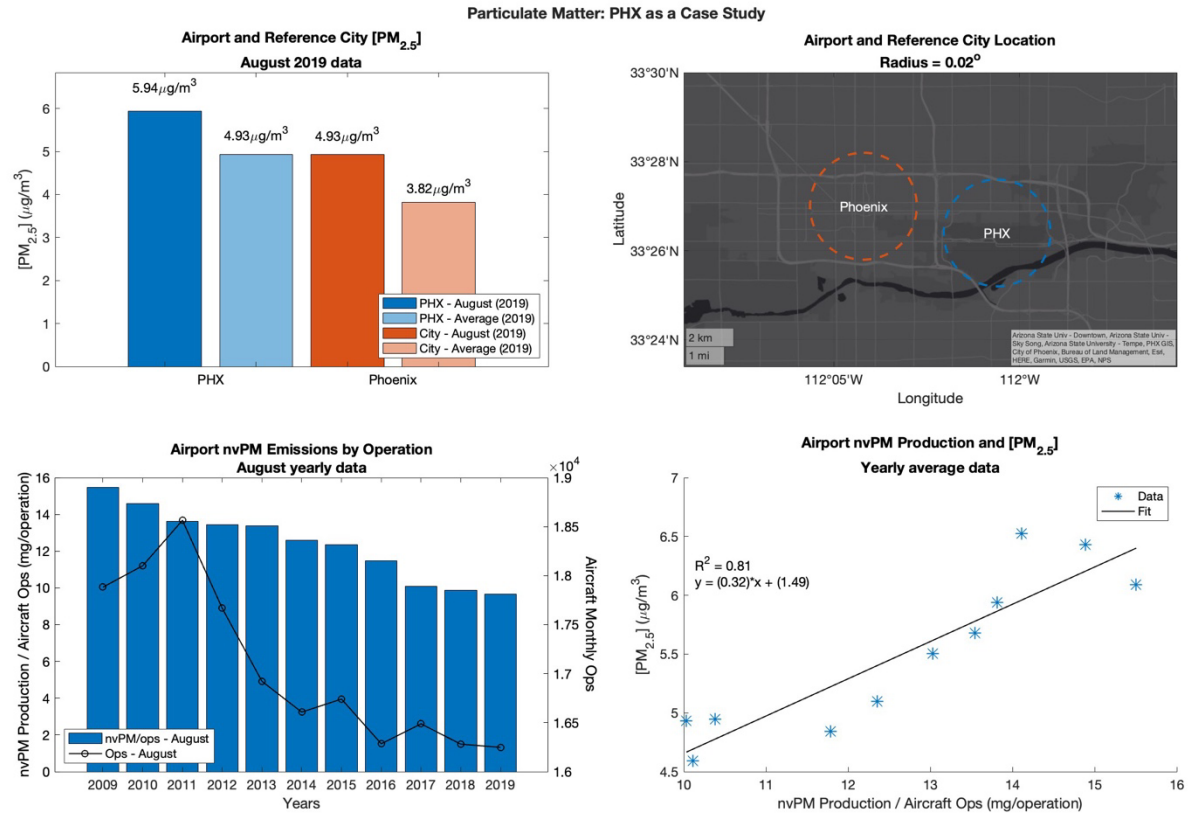

Figure 6: $\mathrm{nvPM_{k,ops}}$and $[\mathrm{PM_{2.5}}]$ at PHX during 2009 and 2019. Here, the results on the upper and lower left plot correspond to August, while the $[\mathrm{PM_{2.5}}]$ were calculated for a resolution radius of 0.02 degrees.

4. Conclusion

Aviation aerosols, both primary and secondary, can influence air quality across various temporal and spatial scales. This work focused on the production of the former category of aerosols, developing an open-source tool that permits visualizing and quantifying local PM production and concentration trends across 30 major U.S. airports between 2009 and 2019. In this process, comparing the results across airports, this work found that there were very distinct temporal and spatial differences between them, especially when examining the potential relationship between nvPM production per operation, $\mathrm{nvPM_{k,ops}}$, and the $[\mathrm{PM_{2.5}}]$. For instance, in BOS, $\mathrm{nvPM_{k,ops}}$ from aircraft alone did not seem to greatly influence the $[\mathrm{PM_{2.5}}]$, while PHL and PHX showed stronger correlations. These results are promising and are worth exploring further; however, this work acts as a preliminary analysis which will require further validation to truly prove or disprove these correlations. First, while $PM_{2.5}$ consists of both primary and secondary aerosol particles, this work only focused on the former category (i.e., BC, OC and sulfur dioxide). Thus, future work should quantify the formation of secondary aerosols subject to local conditions, namely, the presence of NH_3 as well as the local temperature (which influences the deliquescence relative humidity). Second, modeling transport phenomena, in particular wind, would be necessary to properly understand the "fate" of the PM once it is emitted. Third, this work could benefit from incorporating size, mass and number distributions at the different LTO thrust settings, given that particles of different sizes, masses and quantities could have distinct air quality and health impacts. In general, particle sizes increase with the thrust setting, although the number concentration would decrease (Stacey, 2019; Bendtsen, 2021). Finally, another avenue to explore would be including other sources of PM production at airports beyond aircraft engines, such as ground equipment and aircraft APUs (Auxiliary Power Units). Overall, despite the above-mentioned limitations, this work represents a step forwards in reducing barriers for both the general public and policy makers to both understand, in an open way, the local air quality impact of aviation, and also inform the policy that will precisely mitigate this impact.

References

[1] Bendtsen, Katja M., Elizabeth Bengtsen, Anne T. Saber, and Ulla Vogel. "A review of health effects associated with exposure to jet engine emissions in and around airports." *Environmental Health* 20 (2021): 1-21.

[2] BTS. “Form 41 Traffic – T-100 Domestic Segment (U.S. Carriers)”. United States Department of Transportation Bureau of Transportation Statistics (2024).

[3] CAICE. “Introduction to Aerosols”. NSF Center for Aerosol Impacts on Chemistry of the Environment (2020).

[4] Corbin, Joel C., Tobias Schripp, Bruce E. Anderson, Greg J. Smallwood, Patrick LeClercq, Ewan C. Crosbie, Steven Achterberg et al. "Aircraft-engine particulate matter emissions from conventional and sustainable aviation fuel combustion: comparison of measurement techniques for mass, number, and size." *Atmospheric Measurement Techniques* 15, no. 10 (2022): 3223-3242.

[5] Cui, Qiang, Zike Jia, Yujie Liu, Yu Wang, and Ye Li. "24-hour average PM2. 5 concentration caused by aircraft in Chinese airports from Jan. 2006 to Dec. 2023." *Scientific Data* 11, no. 1 (2024): 284.

[6] EASA. “ICAO Aircraft Engine Emission Databank”. European Union Aviation Safety Agency (2024).

[7] Eastham, Sebastian D., Guillaume P. Chossière, Raymond L. Speth, Daniel J. Jacob, and Steven RH Barrett. "Global impacts of aviation on air quality evaluated at high resolution." *Atmospheric Chemistry and Physics* 24, no. 4 (2024): 2687-2703.

[8] Hsu, Hsiao-Hsien, Gary Adamkiewicz, E. Andres Houseman, Jose Vallarino, Steven J. Melly, Roger L. Wayson, John D. Spengler, and Jonathan I. Levy. "The relationship between aviation activities and ultrafine particulate matter concentrations near a mid-sized airport." *Atmospheric Environment* 50 (2012): 328-337.

[9] Hudda, Neelakshi, Tim Gould, Kris Hartin, Timothy V. Larson, and Scott A. Fruin. "Emissions from an international airport increase particle number concentrations 4-fold at 10 km downwind." *Environmental science & technology* 48, no. 12 (2014): 6628-6635.

[10] Hudda, N., M. C. Simon, W. Zamore, D. Brugge, and J. L. Durant. "Aviation emissions impact ambient ultrafine particle concentrations in the greater Boston area." *Environmental science & technology* 50, no. 16 (2016): 8514-8521.

[11] ICAO. “Future of Aviation”. International Civil Aviation Organization (2024).

[12] ICAOb. “Local Air Quality – Overview”. International Civil Aviation Organization (2024).

[13] IPCC. “Aviation and the Global Atmosphere”. Intergovernmental Panel on Climate Change (2024).

[14] Levy, Jonathan I., Matthew Woody, Bok Haeng Baek, Uma Shankar, and Saravanan Arunachalam. "Current and future particulate-matter-related mortality risks in the United States from aviation emissions during landing and takeoff." *Risk Analysis: An International Journal* 32, no. 2 (2012): 237-249.

[15] Lobo, Prem, Donald E. Hagen, Philip D. Whitefield, and David Raper. "PM emissions measurements of in-service commercial aircraft engines during the Delta-Atlanta Hartsfield Study." *Atmospheric Environment* 104 (2015): 237-245.

[16] Prashanth, Prakash, Sebastian D. Eastham, Raymond L. Speth, and Steven RH Barrett. "Aerosol formation pathways from aviation emissions." *Environmental Research Communications* 4, no. 2 (2022): 021002.

[17] Saffaripour, Meghdad, Kevin A. Thomson, Gregory J. Smallwood, and Prem Lobo. "A review on the morphological properties of non-volatile particulate matter emissions from aircraft turbine engines." *Journal of Aerosol Science* 139 (2020): 105467.

[18] Shen, Siyuan, Chi Li, Aaron van Donkelaar, Nathan Jacobs, Chenguang Wang, and Randall V. Martin. "Enhancing Global Estimation of Fine Particulate Matter Concentrations by Including Geophysical a Priori Information in Deep Learning." *ACS ES&T Air* 1, no. 5 (2024): 332-345.

[19] Shirmohammadi, Farimah, Mohammad H. Sowlat, Sina Hasheminassab, Arian Saffari, George Ban-Weiss, and Constantinos Sioutas. "Emission rates of particle number, mass and black carbon by the Los Angeles International Airport (LAX) and its impact on air quality in Los Angeles." *Atmospheric Environment* 151 (2017): 82-93.

[20] Stacey, Brian. "Measurement of ultrafine particles at airports: A review." *Atmospheric Environment* 198 (2019): 463-477.

[21] Woody, Matthew, Bok Haeng Baek, Zachariah Adelman, Mohammed Omary, Yun Fat Lam, J. Jason West, and Saravanan Arunachalam. "An assessment of Aviation's contribution to current and future fine particulate matter in the United States." *Atmospheric Environment* 45, no. 20 (2011): 3424-3433.

[22] Yim, Steve HL, Gideon L. Lee, In Hwan Lee, Florian Allroggen, Akshay Ashok, Fabio Caiazzo, Sebastian D. Eastham, Robert Malina, and Steven RH Barrett. "Global, regional and local health impacts of civil aviation emissions." *Environmental Research Letters* 10, no. 3 (2015): 034001.

[23] Zhou, Limin, Yushan Ni, Huolei Feng, and Xiaowen Hu. "Assessment of predicted aircraft engine non-volatile particulate matter emissions at Hangzhou Xiaoshan International Airport using an integrated method." *Journal of the Air & Waste Management Association* 72, no. 4 (2022): 370-382.